

## Redesign of a Hydraulic Manifold in Additive Manufacturing for Application in a Cleaning and Inspection Robot

Luis Felipe Lopez de Carvalho<sup>1\*</sup>, Luana Seixas Andril Araújo<sup>1</sup>, Valter Estevão Beal<sup>1</sup>, Rafael Tobio Claro<sup>1</sup>, Juan Carlos Romero Albino<sup>1</sup>

<sup>1</sup>SENAI CIMATEC, Industrial Product Development; Salvador, Bahia, Brazil

**A flexible joint riser inspection and cleaning robot must be small and powerful to perform its mission. Hydraulic units are commonly used in submerged operations for power. We designed a custom hydraulic unit as a robot. As the hydraulic manifold is complex, we developed it to be fabricated by additive manufacturing. The objective was to reduce the volume and mass of the hydraulic power unit. We achieved several computational analyzes and analytical methods to validate the designed concept. As a result, we obtained a more compact and lighter structure at the end of the process.**

**Keywords:** Additive Manufacturing. Hydraulic Manifold. Selective Laser Melting. Structural Analysis. Dimensioning.

### Introduction

With the advance of industry 4.0, additive manufacturing (AM) started to gain more space, and its use became common in several sectors. For Keller and Mendrickt (2015) [1], it occurs mainly due to the possibility of producing parts in complex shapes that conventional manufacturing methods cannot obtain.

According to Aboulkhair and colleagues (2019) [2], the AM process has the potential to reduce the design-to-manufacture time of the part by simplifying the production steps (often, the final part is obtained without the need for manufacturing molds and machining process). In addition, there is a reduction in raw materials and materials utilized in components. It means that there is possible to generate more resistant and lighter parts.

In partnership with SENAI CIMATEC, Shell Brasil is developing a robot to clean and remove marine life from flexible joints of rigid risers on floating production platforms. One of the main components that allow the robot to perform its

function is a hydraulic manifold, equipment whose function is to regulate the fluid flow between the pumps and actuators.

The original manifold is a multi-channel structure made of 6061-T6 aluminum, and it has a mass of 3.5 kg [Figure 1(A)]. In this part are coupled five directional valves, a relief valve, a pressure transmitter, a hydraulic accumulator, a motor-pump system, and an air spring [Figure 1(B)]. In addition, the structure was designed to support high loads due to the high power generated by the hydraulic system. A complete structure coupled with the manifold [Figure 1(C) and (D)], with a total height of 372.7 mm and approximately 13.10 kg. The internal channels through which the fluid flows have a diameter of 6 mm and operate under a maximum internal pressure of 60 bar.

Based on this problem, this work presents the redesign of the manifold using the benefits provided by additive manufacturing. As a result, the piece obtained is lighter and occupies a smaller volume than the original, supporting the same mechanical stresses.

### Materials and Methods

Figure 2 summarizes the flowchart with the activities used to redesign the manifold.

We adopted an aluminum alloy with properties like the original model as a material. This choice

Received on 16 June 2022; revised 21 August 2022.

Address for correspondence: Luis Felipe Lopez de Carvalho. Rua Coronel Durval Mattos, 826 - Costa Azul, Salvador - BA - Brazil. Zipcode: 41760-160. E-mail: fellipelopez78@gmail.com. DOI 10.34178/jbth.v5i3.223.

J Bioeng. Tech. Health

2022;5(3):173-179

© 2022 by SENAI CIMATEC. All rights reserved.

**Figure 1.** Original manifold (A), original manifold assembly (B), structures attached to the manifold (C), and view of internal components (D).

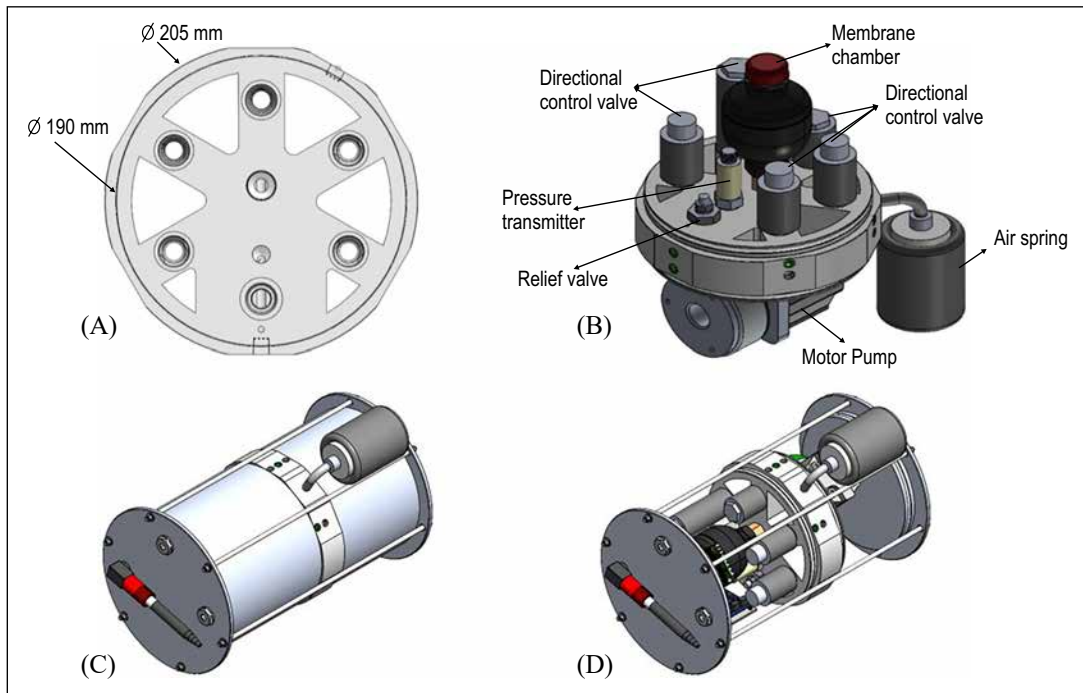
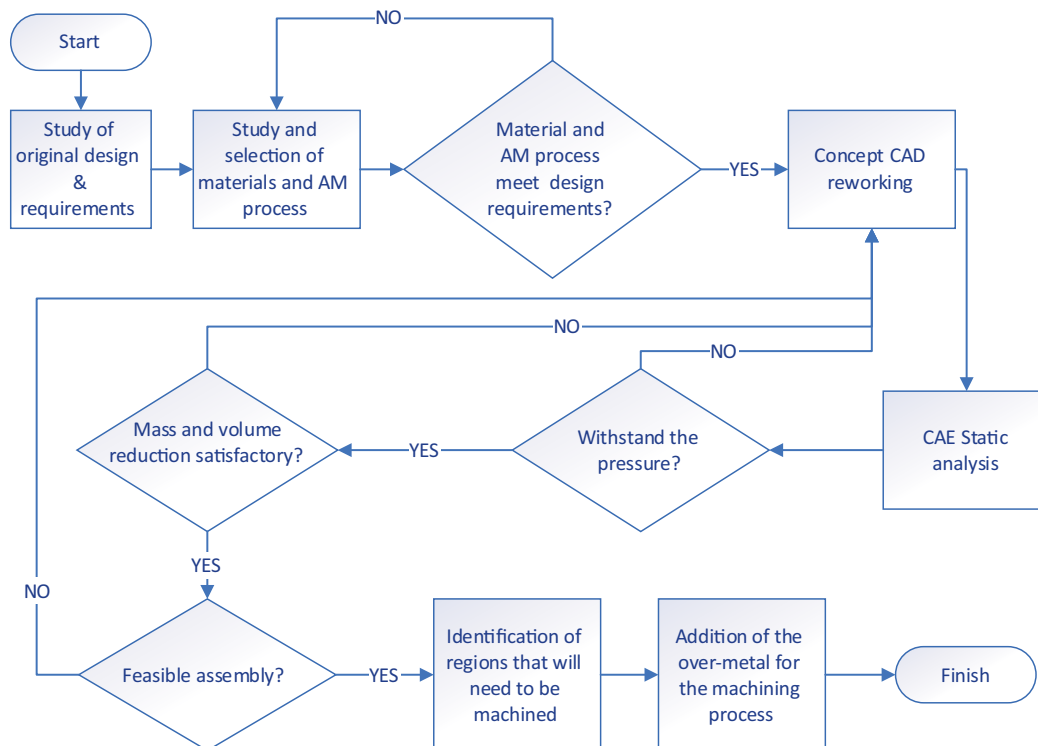


**Figure 2.** Activities' flowchart.



was based on the design requirements since the material support stresses would be high for a polymeric material. Thus, the selected alloy was AlSi10Mg, which has a low density and good corrosion resistance since the part will be submerged in the sea. Furthermore, according to Zygula and colleagues (2018) [3], this material has excellent moldability, low shrinkage, and low melting temperature, making it a good material for additive manufacturing.

The printing method was SLM (Selective Laser Melting). This process uses a high-energy laser beam to melt metal powder in a protective atmosphere, and the molten metal quickly solidifies. A three-dimensional component is eventually formed by repeating this procedure and overlaying it layer by layer. According to Zhang and colleagues (2018) [4], this technology is one of the most promising in the universe of additive manufacturing, as it produces parts with excellent quality and performance, in addition to being possible to reuse the metallic powder that was not cast, reducing the costs.

We used three software for the proposed concept: Solidworks for 3D modeling, Altair Inspire for static analysis and topological optimization, and Ansys for static analysis. Two software performed the analyzes to compare the results. We used the von Mises failure criterion to predict the onset of yielding. After developing the concept, we researched studies of stress concentrators and dimensional calculations. To calculate the diameter of the channels, we consulted Norton (2013) [5] and Shigley (2005) [6] to find the hoop ( $\sigma_\theta$ ) and radial ( $\sigma_r$ ) stresses in thick-walled cylinders. In addition, we consulted ASME [7] for the maximum allowable stress. With the concept defined, it was also necessary to think about the correct order of assembly of the components, ensuring the feasibility of the assembly. Finally, Kamurudin and colleagues (2016) [8] adopted dimensional precision to add the extra metal. The final part will need to go through the machining process for threading and the surface finish required for some areas of the part.

### Material Characterization

The alloy adopted is supplied by the company SLM Solution [9] and has the following chemical composition: 9%-11% Si, 0.55% Fe, 0.05% Cu, 0.45% Mn, 0.20%-0.45% Mg, 0.10% Zn, 0.15% Ti, 0.05% Ni, 0.05% Pb, 0.05% Sn, 0.15% other substances and the remainder aluminum. We used data referring to alloy particles of 60  $\mu\text{m}$  with a laser power of 700 W. After printing, the manufacturer recommends heat treatment to relieve residual stresses by heating the part at 300 °C for 2 hours. Table 1 presents the mechanical properties of the alloy used. In addition, the SLM process has a print rate of 67.9  $\text{cm}^3/\text{h}$ .

**Table 1.** Mechanical properties of AlSi10Mg [9]

Information	Data
Density ( $\text{g}/\text{cm}^3$ )	2.67
Tensile strength (MPa)	261
Yield strength (MPa)	141
Young's modulus (GPa)	59

### Dimensioning of the Internal Manifold Channels

For dimensioning the channels, the hoop ( $\sigma_\theta$ ) and radial ( $\sigma_r$ ) stresses were calculated by the following equations [5, 6]:

$$\sigma_\theta = \frac{p_i r_i^2 p_o r_o^2}{r_o^2 r_i^2} + \frac{r_i^2 r_o^2 p_i p_o}{r^2 (r_o^2 r_i^2)} \quad (1)$$

$$\sigma_r = \frac{p_i r_i^2 p_o r_o^2}{r_o^2 r_i^2} - \frac{r_i^2 r_o^2 p_i p_o}{r^2 (r_o^2 r_i^2)} \quad (2)$$

( $p_i$  and  $p_o$  represent the internal and external pressure,  $r_o$  is the external radius,  $r_i$  is the internal radius, and  $r$  is the radial coordinate).

## **Results and Discussion**

### Manifold Design

The redesign of the original manifold (Figure 1) sought to reduce mass and height. Therefore, we redesigned the proposed structure entirely for

mass reduction. Only functional structures were kept, like the internal channels through which the fluid will flow, the walls of the structure, the valve cavities, the pump support, and hydraulic actuators (Figure 3).

The stresses in the most critical inner channel, with dimensions  $r_i = 3$  mm,  $r_o = 4.75$  mm,  $p_i = 60$  bar, and  $p_o = 5$  bar, were calculated according to Eqs. 1 and 2 (Figure 4).

The maximum von Mises stress obtained in the channels was 16 MPa. This value was compared with the allowable stress according to ASME [7],

whose value is 74.5 MPa. As a result, the stresses in the channels are below the allowed limit. In addition, to support the ducts during the printing process and also to reduce the stress concentration, the fillets suggested by Morgenbrod (Walter D. Pilkey and Deborah F. Pilkey, 2008) [10] were used in the geometry changes arising from the connections of the channels with the cavities. This fillet type is often used on heavy shafts to avoid high stress. There was an increase in the internal diameter of the manifold, from 190 mm to 198 mm, to reduce the structure's height. It allows a better reorganization

**Figure 3.** Proposed manifold concept (A) and its assembly with the main components (B).

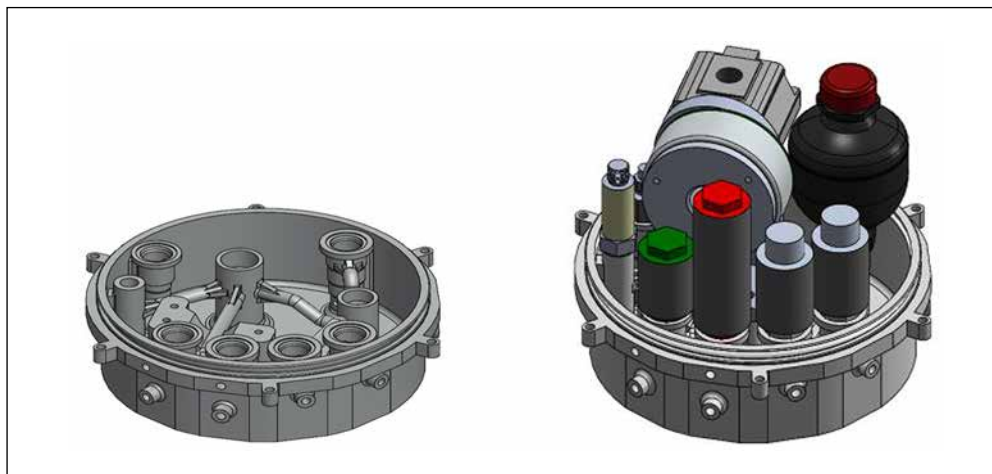
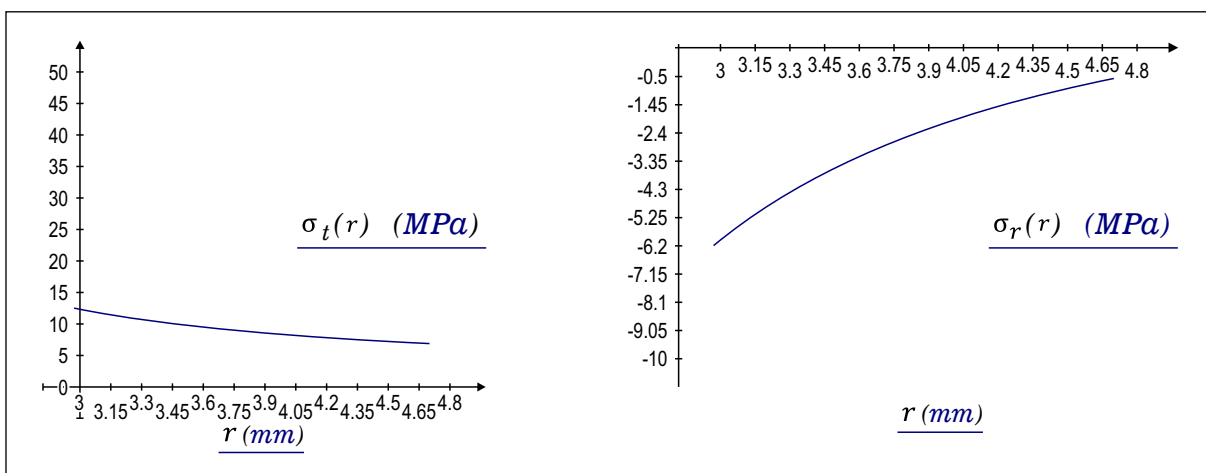


**Figure 4.** Hoop stress (A) and Radial stress (B) are based on the channel radius.



of the components, leaving them on only one side of the structure and eliminating the lower tray and cylinder. In addition, the tie rods now connect directly to the manifold (Figure 5).

We executed a static analysis of the manifold, considering an operating pressure of 60 bar inside the channels. Furthermore, due to the presence of the “air spring”, whose function is to equalize the internal pressure of the manifold with the external pressure (of the water depth of 40 m), an internal and external pressure of 5 bar was adopted in the manifold. As a result, the manifold had a safety coefficient of 1.2, using von Mises as a failure

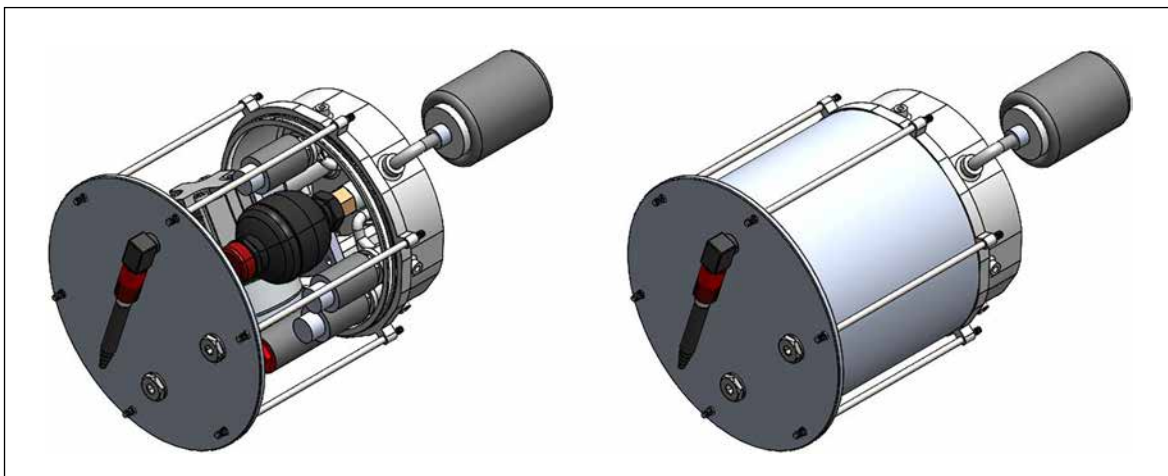
criterion for the onset of yielding. Figure 6 shows the result of the static analysis.

Table 2 compares the original manifold and the manifold proposed in this work. If we consider the assembly complete, we obtained a 30% reduction in height and a 39% reduction in mass with the proposed manifold.

### Machining

After printing the part, it is still necessary to carry out some machining processes to generate the necessary threads and give the recommended surface

**Figure 5.** New assembly structure (view of internal components) (A) and covered (B).



**Figure 6.** Result of static analysis of the manifold (von Mises stress).

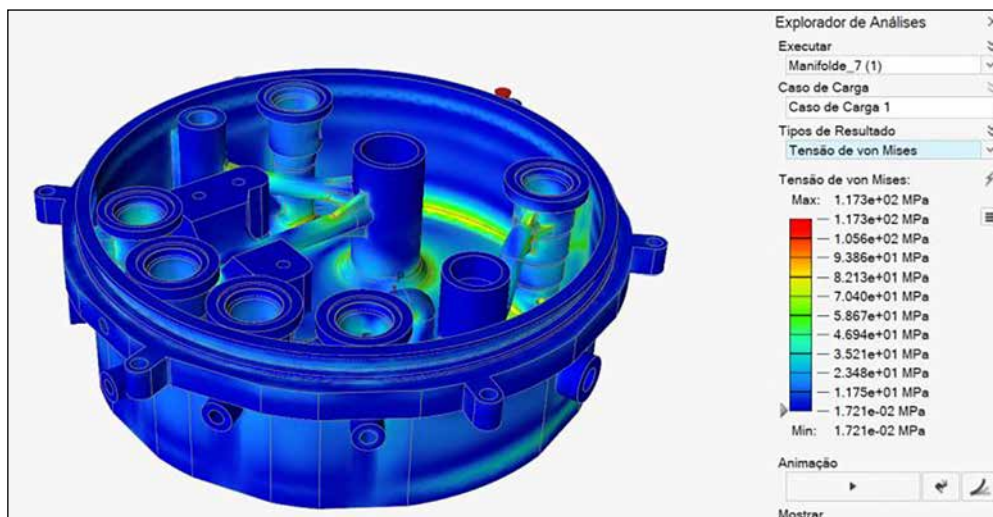




**Table 2.** Models comparison.

Information	Original structure	New AM concept
Manifold Mass (kg)	3.5	1.76
Volume (cm <sup>3</sup> )	Not applicable	659
Complete structure mass (kg)	13.10	8
Complete structure height (mm)	372.7	259.0
Manufacturing time (hr)	Not applicable	9.7

finish for each specific region. For this reason, we tried to add an over-metal in these regions. The over-metal was calculated based on the dimensional accuracy of the SLM printing process and added a safety value, thus ensuring the existence of the amount of material needed for the part to be machined. According to Kamurudin et al. (2016) [8], for cylinders between 10 and 5 millimeters in diameter, there is a variation between 1.3% and 2%. Therefore, a 2.5% diameter surplus was adopted in the regions undergoing the machining process.

## Conclusions

The new manifold withstood the operating demands well, reducing the structure's mass and making it more compact, representing a significant reduction in mass and height. In addition, the redesign reduced the number of components involved in the structure. However, the reduction of mass and volume is not that significant compared to the complete robot. However, this work can be the first step to redesigning other structural components in MA and obtaining more significant results. On the other hand, the assembly of the components of the new manifold became more complex, having to obey a particular order to guarantee the correct fixation of all the elements. However, this difficulty in the assembly does not represent a significant disadvantage. Another disadvantage, this one significant, is the cost of manufacturing the structure. By the traditional method (machining), the cost per part was around 1,500 dollars. With the AM, the cost is around 1,500 to 2,000 dollars, and it will

still be necessary to carry out some machining processes to generate threads and surface finish. The following steps in the project are to obtain more information about the material to perform fatigue analysis on the part, ensuring its good functioning and estimating its lifetime. Later, we expect to print the manifold and perform tests on the prototype.

## Acknowledgments

The authors thank the support of HP Brasil Indústria e Comércio de Equipamentos Eletrônicos Ltda, SENAI CIMATEC, and SHELL do Brasil. This project was funded by HP Brasil using resources based on Law #8.248 of 1982 (Informatics Law).

## References

1. Keller P, Mendricky R. Parameters influencing the precision of SLM production. *MM Science Journal* 2015(out):705-710.
2. Aboulkhair TN. 3D printing of aluminium alloys: Additive manufacturing of aluminium alloys using selective laser melting. *Progress in Materials Science* 2019;106(Dec).
3. Zyguła K, Nosek B, Pasiowiec H, Szysiak N. Mechanical properties and microstructure of AlSi10Mg alloy obtained by casting and SLM technique. *World Scientific News* 2018(July):462-572.
4. Zhang J. A review of selective laser melting of aluminum alloys: Processing, microstructure, property and developing trend. *Journal Of Materials Science & Technology* 2019(Feb):270-284.
5. Norton RL. *Projeto de Máquinas: uma abordagem integrada*. 4. ed. Porto Alegre: Bookman, 2013.
6. Shigley JE, Mischke CR, Budynas RG. *Projeto de Engenharia Mecânica* 7. ed. Porto Alegre: Bookman, 2005.

7. The American Society of Mechanical Engineers. Boiler and pressure vessel code: Section II, Part D: Properties. New York: The American Society of Mechanical Engineers, 2019.
8. Kamarudin K, Wahab MS, Shayfull Z, Ahmed A, Raus AA. Dimensional accuracy and surface roughness analysis for AlSi10Mg produced by selective laser melting (SLM). MATEC Web of Conferences, 2016.
9. SLM Solutions. Al-Alloy AlSi10Mg. Material Data Sheet. Available: [https://www.slm-solutions.com/fileadmin/Content/Powder/MDS/MDS\\_Al-Alloy\\_AlSi10Mg\\_0221.pdf](https://www.slm-solutions.com/fileadmin/Content/Powder/MDS/MDS_Al-Alloy_AlSi10Mg_0221.pdf); Last access: 15/ september/2021.
10. Pilkey WD, Pilkey DF. Peterson's Stress Concentration Factors. 3. ed. United States Of America: John Wiley & Sons, 2007.